Experiments in Fluids (2005) 38: 461–465
DOI 10.1007/s00348-004-0925-9

ORIGINALS

Mingming Wu · John W. Roberts · Mark Buckley

Three-dimensional fluorescent particle tracking at micron-scale using a single camera

Received: 12 September 2004 / Revised: 9 December 2004 / Accepted: 15 December 2004 / Published online: 26 February 2005

Abstract This article reports a new approach to track (x, y, z, t) coordinates of multiple fluorescent particles (diameter range 1–10 μm) simultaneously using a quantitative defocusing method. We find that the defocused image of a 1-μm diameter fluorescent particle formed by the objective lens of a conventional microscope has a bright outer ring due to the spherical aberration of the lens system. The ring radius increases as the particle is moved away from its reference plane and closer to the lens. The reference plane refers to locations of the particle at which the projected image is in focus. The (x, y, z) coordinates of the particle are then inferred from the center location of the image ring as well as the ring radius. The described technique is implemented successfully for obtaining 3D trajectories of swimming *Escherichia coli* cells.

1 Introduction

Three-dimensional tracking of micron-scale particles has become an invaluable tool in diverse scientific disciplines such as microbiology, colloidal science and fluid mechanics. A few examples include the studies of 3D motion of bacteria (Berg 1971; Soni et al. 2003), cell migration (Thar et al. 2000; Guan 2004), interactions between colloidal particles (Dinsmore et al. 2001), and mixing behavior of fluids in a microfluidic device. In the field of fluid mechanics, 3D particle tracking velocimetry (PTV) has had a long history due to its applications in studying technologically important problems such as mixing and stirring. As a result, many imaging techniques, such as stereoscopic imaging (Racca and Dewey 1988), holography (Pu et al. 2000) and quantitative defocusing method (Willert and Gharib 1992), have been developed to track particles in the diameter range of 10 μm–1 mm. Imaging techniques for tracking particles <10 μm have been developed mostly in the field of biology and colloidal science. Early work on 3D tracking of particles in the field of biology has been focused on the single particle tracking (SPT). In the pioneering work of Berg (1971, 2004), a sample containing swimming bacteria (a few μm in size) is mounted on a motorized x-y-z translation stage of a microscope (known as tracking microscope), and the stage is controlled in such a way that a selected bacterium is always in focus. The (x, y, z) coordinates of the bacterium are inferred from the controlling electric signal fed to the x-y-z translation stage. Later work of Soni et al. (2003) uses optical tweezers to track the motion of a single micron size bead bombarded by swimming bacteria. For tracking multiple particles in the same diameter range (1–10 μm) in all three dimensions, the most commonly used imaging technique is scanning confocal microscope. A confocal microscope uses a pin hole to block out the unwanted defocused light, and images the viewing object one point at a time at sub-micron resolution. This technique provides superior spatial resolution and is widely used in biology and colloidal science. The limitation of confocal microscopy is its slow acquisition rate. This is mainly caused by the existence of the pinhole that blocks light both along the incoming and outgoing paths, and greatly impairs the light sensitivity of the imaging system.

We present a novel imaging technique that tracks (x, y, z, t) coordinates of multiple micron scale particles using the spherical aberration rings in the defocused images. The technique has been implemented successfully in a wide field epi-fluorescent microscope. A simplified representation of the imaging system is described in Fig. 1, which is generated from a numerical

M. Wu (✉) · J. W. Roberts
Sibley School of Mechanical and Aerospace Engineering,
Cornell University, Ithaca, NY 14853, USA
E-mail: mw272@cornell.edu

M. Buckley
Department of Physics, Cornell University,
Ithaca, NY 14853, USA

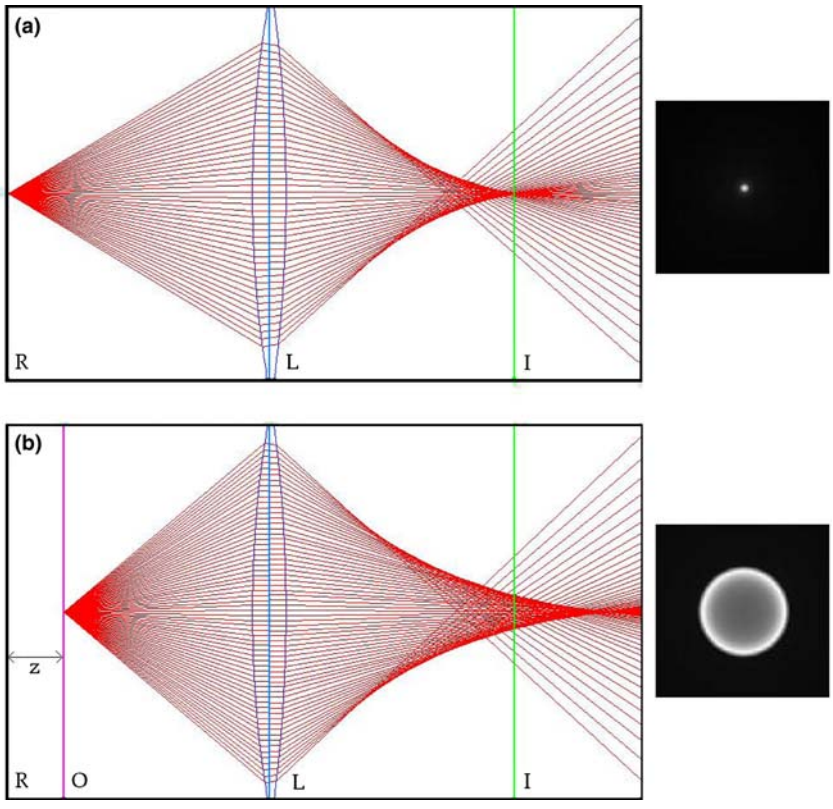

Fig. 1 Schematics of the imaging system. R: reference plane, O: object plane, L: center of lens plane, I: imaging plane. Light rays pass through the lens and form an image in the imaging plane following geometric optics. Images on the *right side* are gray scale image renditions of the light intensity in the imaging plane when the point light source is at the reference plane (**a**) and away from the reference plan (**b**), assuming the optical system possesses rotational symmetry along the optical axis

simulation using geometric optics and a spherical lens. Figure 1 contains four planes of interest: the object plane (O) that marks the location of the particle, the imaging plane (I) that marks the location of imaging sensors, the reference plane (R) that marks locations at which the particle will be focused at the imaging plane, and the lens center plane (L) that marks the center of the two lens surfaces. When a particle sits at the reference plane, a sharp dot image is formed in the imaging plane (Fig. 1a). When the object is moved a distance z away from the reference plane, a ring pattern is formed in the imaging plane (Fig. 1b) due to spherical lens aberration. The ring radius is found to depend solely on z for a specific lens, thus the defocused ring image contains all the information necessary for inferring (x, y, z) coordinates of the object.

2 Experimental work

We first studied the defocused images of a 1-μm diameter green fluorescent bead (Duke Scientific, Palo Alto, CA, USA) using an Olympus upright fluorescent microscope (BX-51). The microscope uses a mercury lamp (Olympus Optical Co., NY, USA), in connection with a Fluorescein filter cube (Chroma Technology Corp, VT, USA). For the data shown below, a 20× objective lens (Olympus UPlanFL NA = 0.50) was used. The fluorescent beads were dry mounted on a glass slide, and then the glass slide was placed on the microscope stage. The beads were first placed at the reference plane. This was achieved by adjusting the vertical position of the beads until they were in focus (see image in Fig. 2 at $z = 0$). The beads were then moved towards the lens using the built-in micrometer (1 μm resolution) of the microscope by a distance z, and images at various z were recorded using a CCD camera (CoolSNAP HQ, Photometrics, CA, USA) (see Fig. 2). The CCD array contains 1,392 pixel×1,040 pixel, and each pixel has a physical dimension of 6.45 μm×6.45 μm. The images such as those shown in Fig. 2 were processed using a Matlab (Mathworks Inc., MA, USA) routine to obtain the radius of the outer bright ring r. A plot of r versus z is shown as a dotted line in Fig. 2. The measuring volume is 418 μm×335 μm×75 μm for the 20× objective. The measuring range in the z direction can be increased by using a brighter light source, lens of higher NA, or a more light sensitive camera. The spatial resolution in the z direction differs depending on the distance between the object and the reference plane. At $z = 60$ μm, the resolution is ~0.48 μm.

It is important to note that the defocused images are not symmetric with respect to the focused plane at $z = 0$. Figure 3 shows a series of images of a 1-μm diameter green fluorescent particle taken along the optical axis at both $+z$ and $-z$ locations. These images have not been contrast enhanced so that one can see the relative light intensity of the images at different defocused planes. It is shown that the bright outer ring disappears when the particle moves away from reference plane into the

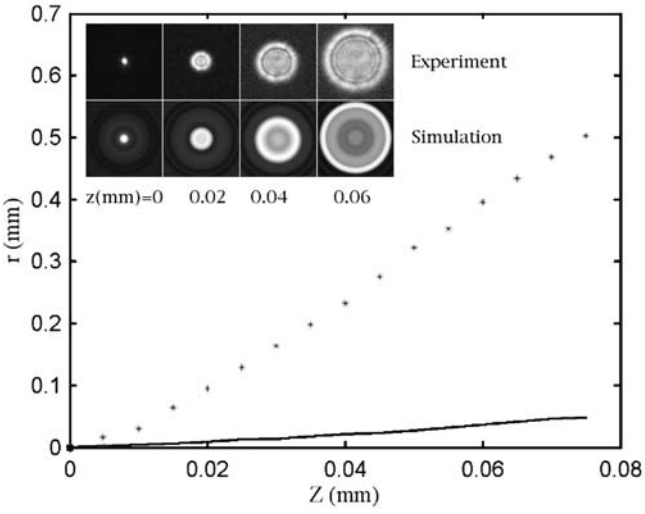

Fig. 2 The ring radius r versus z. *Dotted line* is from experiments using the 20× microscope lens and *connected line* is from numerical simulation using a single spherical lens with 20× magnification. The inserts are images taken at various z locations using the 20× objective microscope lens and from simulation. Each image from the experiment is 1.096 mm×1.096 mm in imaging plane and simulation is 0.085 mm×0.085 mm

negative z region. It is known that diffraction patterns at defocused planes are symmetric with respect to the $z=0$ plane (Cagnet et al. 1962); Fig. 3 indicates that the defocused images we observed here are dominated by the spherical aberration in the lens system.

To test the described method in a real experimental setting, we tracked bacteria swimming in a nutrient limited water bath. Wildtype *Escherichia coli*, strain RP437 from Dr. Parkinson's lab at University of Utah, was chosen due to its well characterized motile behavior. The bacteria were first transformed with a DNA plasmid which expresses green fluorescent protein (GFP) constitutively. As a result, RP437 carrying this plasmid are continuously fluorescent when excited by light with 488 nm wavelength. The bacteria were then grown in a LB media (nutrient rich) overnight at 30 °C, and diluted in a M9 (nutrient limited) media 30 min before the experiment. A sample of ~15 μl was placed between two glass slides and separated by an O-ring. The distance between the two glass slides was typically 1.5 mm and the microscope stage was adjusted in such a way that the reference plane was at 500 μm below the lower side of the top slide. A sequence of images was then taken while the time duration of the sequence was recorded using a stop watch. Shown in Fig. 4a is an unprocessed image in an image series. Each image has 696 pixel×520 pixel, and the time between consecutive images is 0.752 s. The different ring sizes indicate the different z locations of the bacteria. The (x, y, z) coordinates of each bacteria in a given image were obtained by a Matlab routine. Figure 4b shows trajectories of several swimming bacteria. The running and tumbling motion known to this type of bacteria is clearly displayed in Fig. 4b.

3 Numerical work

It is known that rings in the defocused imaging plane are caused by both diffraction and spherical lens aberration (Inoué and Spring 1997). To decouple the contribution of these two terms to the final images in the defocused

Fig. 3 Raw images taken at different planes along the optical axis z using the 20× objective lens. From left to right, $z=-30$, -20, -10, 0, 10, 20, and 30 μm, respectively. Each image is 100 pixels×100 pixels, which corresponds to 0.645 mm×0.645 mm in the imaging plane

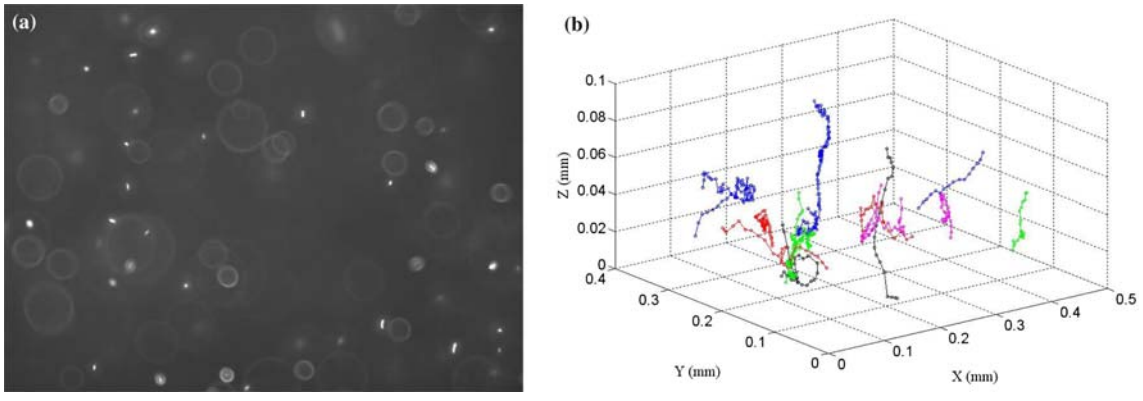

Fig. 4 **a** An unprocessed image from the image series, each image is 696 pixel×520 pixel which corresponds to 0.449 mm×0.336 mm in the object plane. **b** 3D trajectories of bacteria from the image series

plane as well as to understand the underlying mechanism behind the ring shape images, we carried out a numerical simulation based on geometric optics in a diffraction free optical system. In the simulation, a single spherical lens was used, and results indicated that the bright outer ring in the defocused image of a point light source formed by a microscope objective lens was caused by spherical aberration of the lens (Fig. 5).

The simulation was carried out in a 3D setting assuming the system possesses axisymmetric symmetry around the optical axis. Light rays from a point light source are projected to the lens at equally spaced angles (see Fig. 1). They then pass through the two surfaces of the lens according to Snell's law until they hit the imaging plane. The line density of the rays hitting the imaging plane is used as the light intensity of the image. The lens is made of two spherical surfaces with radius R_1 and R_2. The simulator was first tested against the Lensmaker's equation, which can be written as: $(n-1)(1/R_1-1/R_2)=1/f$. Here R_1 and R_2 are the radii of the two lens surfaces, $n=1.51$ is the optical index of the lens, and f is the focal length of the resultant lens. Several thin lenses with different radii were programmed into the simulator and the focal point was determined by moving the point light source along the optical axis until the light rays leaving the lens were parallel. The simulator's results confirmed the Lensmaker's law.

The first simulation was carried out modeling the 20× microscope objective. As the detailed construction of the objective lens is unknown to us, we started with a single spherical lens with $R_1=3.0$ mm and $R_2=6.44$ mm, producing a focal length of 5.15 mm. The distance from the reference plane to lens center is chosen to be 5.41 mm and the distance between the lens center and the imaging plane is 109.4 mm. The magnification of the image to object is $109.4/5.41=20.2$, which is slightly above 20. The results of the simulation are shown in Fig. 2. It can be seen that images from numerical simulation capture the essential feature of the defocused images from experiments, and a bright outer ring is clearly visible in each of the defocused images. The r versus z curves from experiment and simulation follow the same trend; however, the ring radius from the numerical simulation is about 13 times smaller than those from experiments. This is likely caused by the multi-lens system that a microscope objective has in comparison to the single lens system from the numerical simulation.

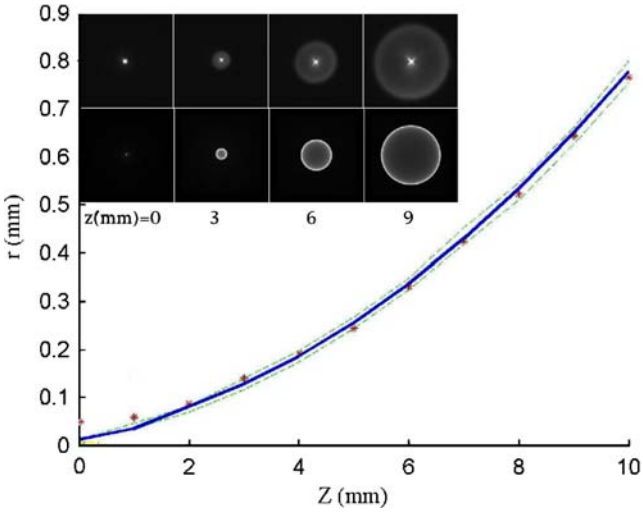

Fig. 5 Ring radius of the defocused images r versus z from experiment (*dotted line*) and numerical simulation (*connected line*). The two upper/lower dashed lines are from numerical simulation using the upper/lower bound of z from experiments. The inserts are defocused images at various z locations from experiment (*upper row*) and numerical simulation (*lower row*). Each image is 1.33 mm×1.33 mm

In order to further demonstrate quantitatively that the ring shape image in the defocused plane can indeed be explained by geometric optics, we did a proof of principal experiment using a spherical lens with known dimensions. In this experiment, we used a spherical glass lens (13K7, optical index = 1.51, ThorLab, NJ, USA) with $R_1=24.5$ mm, $R_2=24.5$ mm, and focal length 25.4 mm. The point light source was provided by a 5-μm diameter pinhole (ThorLab) together with a halogen light source (Model 20, Stocker Yale, NH, USA). The light passed through the spherical lens and formed an image directly on a CCD array. The optical system is diffraction free since there is no restriction in the optical path. In numerical simulation, we used point light source, and a lens with the same dimension as the one described above. In the experiment, the distance between the reference plane to the lens center was 52.1 ± 0.2 mm and the distance between the lens center to the image plane was 50.5 ± 0.3 mm. In the numerical simulation, we used 50.5 mm for the distance from lens center to the image plane. Figure 4 shows that the ring shape images are formed in both experiments and simulation. The bright dot in the center of the experimental images is caused by the finite size of the light source. The r versus z curve from numerical simulation agrees well with that of experiment.

4 Summaries and discussions

In summary, we have demonstrated that the (x, y, z) coordinates of multiple micron-scale fluorescent particles can be tracked simultaneously using a conventional epi-fluorescent microscope and a CCD camera, in which the distance between the particle and the objective lens is inferred from the defocused images. The ring shape images in the defocused planes are studied both experimentally and numerically. Experimentally, the defocused images contain a set of rings as a result of diffraction and spherical aberration of the lens system. Numerical simulation allows us to decouple the contribution of these two, and demonstrated that the bright outer ring in the defocused image is caused by spherical

aberration of the lens system. The size of the bright outer ring changes monotonically with z , thus can be used to infer the z dimension. Using an Olympus epi-florescent microscope, the 3D trajectories of bacteria (size 1–3 μm) swimming in a bath are obtained. It should be noted, to date, 3D tracking of microorganisms that are less than 10 μm in size has only been possible for single cell tracking (Berg 1971; Soni et al. 2003).

The described technique provides a 3D imaging method for tracking fast moving micron scale particles. In contrast to confocal microscope, our technique uses a wide field epi-fluorescent microscope and collects all light. In addition, it probes a volume instead of a point of the viewing object at a given time. Such optical arrangement allows for better light sensitivity and higher acquisition rate over confocal microscope. The disadvantage is that it only works with dilute suspension of particles while confocal microscope can track densely packed particles.

Three-dimensional particle tracking using defocused images is not limited to the particle size range of 1–10 μm in diameter. Speidel et al.(2003) demonstrated that single nano-particles can be tracked using the defocused images at sub-nanometer resolution in all three dimensions. The present work extended the SPT of nano-particles of Speidel et al. (2003) to multi-particle tracking at micron scale, and further investigated the underlying mechanism of the ring images observed in the defocused planes. The ability to decouple diffraction with spherical aberration using numerical simulation allows us an ability to better design the next generation lens system, where the aberration ring can be used to probe the third dimension. It is clear that diffraction needs to be eliminated or minimized for achieving better light sensitivity in the next generation tracking system. In addition, we are in the process of developing a software package to achieve 3D micro PTV, where a 3D velocity field can be obtained using the technique described here. For particle size range 10 μm–1 mm, Willert and Gharib (1992) have developed a 3D tracking mechanism via the quantitative use of the defocused images, where a modified three hole aperture was used in conjunction with a commercial video lens and a CCD camera. The method has been proven successful in tracking particles >10 μm as well as rising air bubbles of a few millimeter in diameter (Willert and Gharib 1992; Wu and Gharib 2002).

Acknowledgements We would like to thank Professor DeLisa from the Chemical and Biomolecular Engineering Department at Cornell University for providing us with bacteria samples. This work is supported by the National Science Foundation (CTS-0121340), and a startup fund from the Physics Department at Cornell University.

References

Berg HC (1971) How to track bacteria. Rev Sci Instrum 42:868
Berg HC (2004) *E. Coli* in motion. Springer, Berlin Heidelberg New York
Cagnet M, Francon M, Thrierr JC (1962) Atlas of optical phenomena. Springer, Berlin Heidelberg New York
Dinsmore AD, Weeks ER, Prasad V, Levitt AC, Weitz DA (2001) Three-dimensional confocal microscopy of colloids. Appl Opt 40:4152
Guan J-L (2004) Cell migration: developmental methods and protocols. Humana, Totowa
Inoué S, Spring KR (1997) Video microscopy, 2nd edn. Plenum, New York
Pu Y, Song X, Meng H (2000) Holographic PIV for diagnosing particulate flows. Exp Fluids 29:S117
Racca RG, Dewey JM (1988) A method for automatic particle tracking in a three-dimensional flow field. Exp Fluids 6:25
Soni GV, Jaffar Ali BM, Hatwalne Y, Shivashankar GV (2003) Single particle tracking of correlated bacterial dynamics. Biophys J 84:2634
Speidel M, Jonas A, Florin E (2003) Three-dimensional tracking of fluorescent nanoparticles with subnanometer precision by use of off-focus imaging. Opt Lett 28:69
Thar R, Blackburn N, Kuhl M (2000) A new system for three-dimensional tracking of motile microorganisms. Appl Environ Microbiol 66:2238
Willert CE, Gharib M (1992) Three-dimensional particle imaging with a single camera. Exp Fluids 12:353
Wu M, Gharib M (2002) Experimental studies on the shape and path of small air bubbles rising in clean water. Phys Fluids 14:L49